



This discussion paper is/has been under review for the journal Hydrology and Earth System Sciences (HESS). Please refer to the corresponding final paper in HESS if available.

Climate elasticity of streamflow revisited – an elasticity index based on long-term hydrometeorological records

V. Andréassian¹, L. Coron^{1,*}, J. Lerat², and N. Le Moine³

¹Irstea, Hydrosystems and Bioprocesses Research Unit (HBAN), Antony, France

²Bureau of Meteorology, Canberra, Australia

³UPMC, Paris, France

*now at: EDF-DTG, Toulouse, France

Received: 6 March 2015 – Accepted: 17 March 2015 – Published: 1 April 2015

Correspondence to: V. Andréassian (vazken.andreassian@irstea.fr)

Published by Copernicus Publications on behalf of the European Geosciences Union.

HESSD

12, 3645–3679, 2015

Climate elasticity of
streamflow revisited

V. Andréassian et al.

Title Page

Abstract

Introduction

Conclusions

References

Tables

Figures

⏪

⏩

◀

▶

Back

Close

Full Screen / Esc

Printer-friendly Version

Interactive Discussion



Abstract

We present a new method to derive the empirical (i.e., data-based) elasticity of streamflow to precipitation and potential evaporation. This method, which uses long-term hydrometeorological records, is tested on a set of 519 French catchments.

We compare a total of five different ways to compute elasticity: the reference method first proposed by Sankarasubramanian et al. (2001) and four alternatives differing in the type of regression model chosen (OLS or GLS, univariate or bivariate). We show that the bivariate GLS regression is the most robust solution, because it accounts for the co-variation of precipitation and potential evaporation anomalies. We also compare empirical elasticity estimates with theoretical estimates derived analytically from the Turc–Mezentsev formula.

Empirical elasticity offers a powerful means to test the extrapolation capacity of those hydrological models that are to be used to predict the impact of climatic changes.

1 Introduction

1.1 About hydrological elasticity

In a context of growing uncertainty on water resources due to climate change, simple tools able to provide robust estimates of this impact are essential to support policy and planning decisions. Streamflow elasticity is one such tool: it describes the sensitivity of the changes in streamflow related to changes in a climate variable (Schaake and Liu, 1989). $\varepsilon_{Q/X}$, the elasticity of streamflow Q to a climate variable X is defined by the following equation:

$$\Delta Q / \bar{Q} = \varepsilon_{Q/X} \Delta X / \bar{X} \quad (1)$$

where \bar{Q} and \bar{X} are the long-term average value of streamflow and the climatic variable, respectively, and the operator Δ indicates the difference or change. $\varepsilon_{Q/X}$ is nondimen-

HESSD

12, 3645–3679, 2015

Climate elasticity of streamflow revisited

V. Andréassian et al.

Title Page

Abstract

Introduction

Conclusions

References

Tables

Figures

⏪

⏩

◀

▶

Back

Close

Full Screen / Esc

Printer-friendly Version

Interactive Discussion



sional [%/%], because it is a ratio between two relative (and thus already nondimensional) quantities. One can also define elasticity as the ratio between two absolute quantities and, provided both quantities are expressed in the same unit (for example, mm yr^{-1} for streamflow, precipitation or potential evaporation), it would still be a nondimensional ratio [$\text{mm yr}^{-1}/\text{mm yr}^{-1}$]. We will name this absolute elasticity $e_{Q/X}$, defined as:

$$\Delta Q = e_{Q/X} \Delta X \quad (2)$$

Table 1 summarizes the notations used in this paper.

1.2 Past studies on elasticity in hydrology

1.2.1 Theoretical (model-based) studies

Most of the studies on elasticity are *theoretical*, in the sense that they are based on flows simulated by a hydrological model fed with different inputs. There are many examples of such theoretical studies. Nemeč and Schaake (1982) used the Sacramento model, Vogel et al. (1999) used the linear regression coefficients of annual streamflow models, Sankarasubramanian et al. (2001) used the abcd model, Niemann and Eltahir (2005) used a purpose-built model and Chiew (2006) used the SIMHYD and AWBM models. The most widely used model in elasticity studies is the long-term water balance formula first proposed by Turc and Mezentsev (Mezentsev, 1955; Turc, 1954) (see Sect. 3.2). This formula (sometimes improperly confused with Budyko's formula) was used in elasticity studies by Dooge (1992), Arora (2002), Sankarasubramanian et al. (2001), Yang et al. (2008), Potter and Zhang (2009), Yang and Yang (2011), Donohue et al. (2011) and Yang et al. (2014), among others.

Title Page

Abstract

Introduction

Conclusions

References

Tables

Figures

◀

▶

◀

▶

Back

Close

Full Screen / Esc

Printer-friendly Version

Interactive Discussion



1.2.2 Empirical (data-based) studies

Only a few of the published elasticity studies are *empirical*. By empirical, we mean that they use measured data (for different sub-periods) to evaluate the climate elasticity of streamflow. To our knowledge, Sankarasubramanian et al. (2001) were the first to publish a method based on the median of annual flow anomalies to compute elasticity, later used by Chiew (2006). Potter et al. (2010) analyzed concomitant reductions of precipitation and streamflow in the Murray–Darling basin over three major historic droughts, and Potter et al. (2011) suggested computing elasticity as a multiple linear regression linking annual transformed streamflow values to annual precipitation and temperature anomalies.

1.2.3 Difference between theoretical (model-based) and empirical (data-based) elasticity assessments

To clarify the differences existing between theoretical and empirical elasticity computing approaches, we have listed the key characteristics of both methods in Table 2. The most important problem stems from the co-variation of potential evaporation (or temperature) and precipitation: Chiew et al. (2014) underline that “because of the inverse correlation between rainfall and temperature, any effect from the residual temperature on streamflow is much less apparent than the direct effect of (the much more variable) rainfall.” Note that the use of model simulations to compute streamflow elasticity circumvents this problem.

However, there remains what we consider to be a major disadvantage: since all hydrological models are a simplification of reality, using them to predict changes requires some type of initial validation on empirical (observed) data. Indeed, we have recently compared (see Fig. 9a in Coron et al., 2014) the ability of three models of increasing complexity to reproduce the variations in water balance equilibrium over 10-year-long periods and shown that all three models tested had a tendency to underestimate observed changes.

HESSD

12, 3645–3679, 2015

Climate elasticity of streamflow revisited

V. Andréassian et al.

Title Page

Abstract

Introduction

Conclusions

References

Tables

Figures

◀

▶

◀

▶

Back

Close

Full Screen / Esc

Printer-friendly Version

Interactive Discussion



In this paper, we will focus on identifying the most robust approach to compute empirical elasticity. Then we will compare the results obtained by this method with the theoretical elasticity of the Turc–Mezentsev water balance formula. This comparison will only aim at illustrating the difference between the two approaches, since there is no reason to consider one or the other as the “true” reference.

1.3 Scope of the paper

In this paper, we test four alternative approaches to compute the empirical streamflow elasticity, which we compare over a large catchment set to the approach first suggested by Sankarasubramanian et al. (2001). In Sect. 2, we present the data set of 519 French catchments on which this study is based. Section 3 gives a short overview on the possible graphical representations of catchment elasticity and the methods used to quantify empirical elasticity. Section 4 presents a preliminary selection of the formulas, focusing on the distinction between univariate and bivariate methods. Then Sect. 5 presents a regional analysis of streamflow elasticity to precipitation and potential evaporation over France. Last, the conclusion identifies a few perspectives for further work.

2 Catchment dataset

Figure 1 presents the 519 catchments analyzed for these studies.

Long series of continuous daily streamflow and precipitation were available over the 1976–2006 period. The data set encompasses a variety of climatic conditions (oceanic, Mediterranean, continental, mountainous). Precipitation data was provided by Météo France as a gridded product, based on a countrywide interpolation of rain gage data (SAFRAN product). As far as potential evaporation data is concerned, we used the Penman–Monteith equation (Allen et al., 1998) in this paper.

Title Page

Abstract

Introduction

Conclusions

References

Tables

Figures

⏪

⏩

◀

▶

Back

Close

Full Screen / Esc

Printer-friendly Version

Interactive Discussion



To illustrate the issues raised this paper, we will use the catchment of the River Brèze at Meyrueis. This 36 km² catchment located in the south of France has a good quality stream-gaging station and a long observation series.

3 A review of methods to assess streamflow elasticity

3.1 Graphical assessment of elasticity

Nemec and Schaake (1982) introduced the classical sensitivity plots showing the changes in streamflow (or in some streamflow-based characteristics) as a function of percent change in precipitation (Fig. 2). Their approach consisted in assessing streamflow elasticity over the whole modeling period by gradually changing the model inputs individually. If the hydrological model behavior is free from thresholds or strong hysteresis effects, this method produces a set of parallel curves such as those shown in Fig. 2.

Wolock and McCabe (1999) used a similar graph (Fig. 3), but replaced the percent changes with the absolute changes (plotting $e_{Q/X}$ instead of $\varepsilon_{Q/X}$): in this paper, we will follow their example, but replace the model-based results with observations.

The graphs used herein describe *empirical elasticity*: they are based on hydrological data only and require a sub-sampling of long-term records, i.e., distinguishing a number of sub-periods. Therefore, a point is apparent for each of these sub-periods. Figure 4 presents an example in which ΔQ is plotted as a function of either ΔP or ΔE_0 .

To represent the co-variations of ΔQ with both ΔP or ΔE_0 simultaneously, we need either a three-dimensional graph or a graph based on isolines (see Fu et al., 2007). Figure 4c presents an example using a color code. This graph is particularly useful because the values of ΔP and ΔE_0 are often correlated (Chiew et al., 2014), which may make the two-dimensional representations misleading.

The graphical representation of empirical elasticity shown in Fig. 4 allows looking at data without formulating an arbitrary modeling choice. The only convention lies in

Title Page

Abstract

Introduction

Conclusions

References

Tables

Figures

◀

▶

◀

▶

Back

Close

Full Screen / Esc

Printer-friendly Version

Interactive Discussion



the duration of the sub-periods. Here, we chose a duration of 10 years in order to obtain contrasted yet representative periods. Figure 5 illustrates the changes induced by a change in this duration. It is reassuring to see that similar trends are observed for a wide range of period lengths. The relationship between the different variables does not remain absolutely identical, however, and there is clearly a trade-off between a longer duration, which ensures that the relationships are close to their long-term value, and a lower number of points, which reduces the confidence in the trend displayed by the plot.

3.2 Reference method for theoretical elasticity assessment: the Turc–Mezentsev formula

Most of previous studies used a model-based definition of elasticity, and several of them used the Turc–Mezentsev formula (Mezentsev, 1955; Turc, 1954). The interested reader can refer to Lebecherel et al. (2013) for an historical review on this formula, which is given by:

$$Q = \Psi(P, E_0) = P - \frac{P}{\left(1 + \left(\frac{P}{E_0}\right)^n\right)^{\frac{1}{n}}} = P - (P^{-n} + E_0^{-n})^{-\frac{1}{n}} \quad (3)$$

with Q – long-term mean average flow (mm yr^{-1}), P – long-term mean average precipitation (mm yr^{-1}), E_0 – long-term mean average potential evaporation (mm yr^{-1}). n is the only free parameter of the formula. Here, we followed Le Moine et al. (2007) and used a fixed value $n = 2.5$.

Partial derivatives of the Turc–Mezentsev formula are easily computed, they are given in Eqs. (4) and (5). They allow computing the theoretical value of the precipi-

Title Page

Abstract

Introduction

Conclusions

References

Tables

Figures

◀

▶

◀

▶

Back

Close

Full Screen / Esc

Printer-friendly Version

Interactive Discussion



tation and potential evaporation elasticity directly for each catchment.

$$\frac{\partial Q}{\partial E_0} = \Psi'_P(P, E_0) = - \left(1 + \left(\frac{E_0}{P} \right)^n \right)^{-\frac{n+1}{n}} \quad (4)$$

$$\frac{\partial Q}{\partial P} = \Psi'_{E_0}(P, E_0) = 1 - \left(1 + \left(\frac{P}{E_0} \right)^n \right)^{-\frac{n+1}{n}} \quad (5)$$

3.3 Alternative methods for empirical streamflow elasticity assessment

We will now focus on data-based methods assessing empirical elasticity. Long-term series of streamflow and catchment climate are required. Before introducing the methods compared in this paper, let us introduce the notation $\Delta X_i^{(M)} = X_i^{(M)} - X^{(LT)}$ denoting the departure (anomaly) of a variable X computed over a period of M years starting from year i vs. the long-term average $X^{(LT)}$ computed over the entire period.

Five methods will be compared in this paper, all listed in Table 3.

3.3.1 Nonparametric method

This method computes an annual time-series of relative streamflow anomalies (i.e., differences with the long-term mean) and then uses the median of these values as an elasticity estimator:

$$\begin{cases} e_{Q/P}^{(M)} = \text{median} \left(\frac{\Delta Q_i^{(M)}}{\Delta P_i^{(M)}} \right) \\ e_{Q/E_0}^{(M)} = \text{median} \left(\frac{\Delta Q_i^{(M)}}{\Delta E_{0i}^{(M)}} \right) \end{cases} \quad (6)$$

This method is similar to the one advocated by Sankarasubramanian et al. (2001) except that they used it to compute the relative rather than the relative elasticity (see Table 1). In addition, Sankarasubramanian et al. (2001) applied the method to yearly data only, whereas we used sub-periods ranging from 1 to 25 years in this study.

Title Page

Abstract

Introduction

Conclusions

References

Tables

Figures

◀

▶

◀

▶

Back

Close

Full Screen / Esc

Printer-friendly Version

Interactive Discussion



3.3.2 Regression methods quantifying precipitation and potential evaporation elasticities (OLS or GLS estimates) independently

These methods compute elasticity as either an ordinary least-square (OLS) or generalized least-square (GLS) solution (Johnston, 1972) of the regression models detailed in Table 4.

The parameters of the GLS regression were inferred by maximizing the log-likelihood function associated with this model:

$$L\left(\left\{\Delta Q_i^{(M)}\right\},\left\{\Delta X_i^{(M)}\right\}\middle|e_{Q/X}^{(M)},\sigma,\alpha\right)=-\frac{k}{2}\log(2\pi)-k\log(\sigma)-\frac{1}{2}\log(1-\alpha^2)-\frac{1}{2\sigma^2}\left(\left(1-\alpha^2\right)\omega_1^2+\sum_{i=2}^k\left(\omega_i-\alpha\omega_{i-1}\right)^2\right) \quad (7)$$

where k is the number of sub-periods. The optimization was performed with the Nelder–Mead algorithm (Nelder and Mead, 1965) using the ordinary least-square solution (OLS) as a starting point (i.e., the solution of the same regression model with $\alpha = 0$). The validity of the model assumptions was checked (see Appendix) by computing the Shapiro–Wilks test (with an expected p value greater than 0.05) and Durbin–Watson statistic (with an expected value greater than 1) from the series of innovations $\hat{\delta}_i$ (Eqs. 8 and 9).

$$\hat{\delta}_i = \hat{\omega}_i - \alpha \hat{\omega}_{i-1} \text{ if } i > 1 \text{ and } \hat{\delta}_1 = \hat{\omega}_1 \quad (8)$$

$$\hat{\omega}_i = \Delta Q_i^{(M)} - e_{Q/X}^{(M)} \Delta X_i^{(M)} \quad (9)$$

Unlike the OLS solution, the distribution of the elasticity values obtained with this approach does not have a closed form. As a result, the significance of the regression's coefficients was assessed with a bootstrap approach as follows:

1. The GLS model was fit with the maximum likelihood approach first. This allowed computing the series of innovations δ_j .

Title Page

Abstract

Introduction

Conclusions

References

Tables

Figures

◀

▶

◀

▶

Back

Close

Full Screen / Esc

Printer-friendly Version

Interactive Discussion



2. The innovations $\{\delta_i\}_{i=2,\dots,n}$ were resampled with replacement to form a new series of bootstrapped innovations $\{\delta_i^*\}_{i=2,\dots,n}$. The first innovation δ_1^* of this series was set to ω_1 .
3. The bootstrapped innovations were used to generate a new series of bootstrapped observations $\Delta Q_i^{(M)*} = e_{Q/X}^{(M)} \Delta X_i + \sum_{i=1}^n \delta_i^* \alpha^i$.
4. Finally the GLS model was fit with the maximum likelihood approach using the bootstrapped observations leading to new values of the GLS parameters.

Steps (3) and (4) were repeated 1000 times and the 2.5 and 97.5 % percentiles of the GLS parameters were derived from the empirical distribution formed with the 1000 parameter samples. A parameter was considered as significantly different from zero if both the 2.5 and 97.5 % percentiles were either strictly positive or negative.

3.3.3 Methods quantifying precipitation and potential evaporation elasticities (OLS or GLS estimates) simultaneously

These methods (OLS or GLS) quantify precipitation and potential evaporation elasticities *simultaneously* by looking for the GLS solution of a regression model with the same statistical assumptions as above (see Table 5).

The strength of the bivariate method obviously lies in the fact that it accounts for the cross-correlation of ΔP and ΔE_0 values. The method used for inferring the parameter values and their significance was identical to the method described above.

Note that for the sake of consistency with the GLS models, the uncertainty in the OLS parameters was assessed with the bootstrap approach.

[Title Page](#)[Abstract](#)[Introduction](#)[Conclusions](#)[References](#)[Tables](#)[Figures](#)[I◀](#)[▶I](#)[◀](#)[▶](#)[Back](#)[Close](#)[Full Screen / Esc](#)[Printer-friendly Version](#)[Interactive Discussion](#)

4 Selection of the best method to compute empirical streamflow elasticity

4.1 Assessing the capacity of the five methods to compute the empirical elasticity of a synthetic data set

As a first step to compare the merits of the different regression models presented in the previous section, the elasticity estimation was conducted with synthetic streamflow data generated from the Turc–Mezentsev formula, where the parameter n was set at 2.5 (Le Moine et al., 2007). The advantage of using synthetic flow here is that we know the exact (i.e., analytical) solution for elasticity, and this identifies the drawbacks of some of the methods compared.

For this test, the observed streamflow anomalies $\Delta Q_i^{(M)}$ were replaced by the estimates $\Delta \tilde{Q}_i^{(M)} = \Psi(P_i^{(M)}, E_{0i}^{(M)}) - \Psi(P^{(LT)}, E_0^{(LT)})$ where Ψ is given in Eq. (3). The empirical elasticity values were subsequently compared with the exact values $\Psi'_P(P^{(LT)}, E_0^{(LT)})$ and $\Psi'_{E_0}(P^{(LT)}, E_0^{(LT)})$ given in Eqs. (4) and (5), respectively. The performance of each regression model was judged according to the absolute bias B and root mean square error (RMSE) R :

$$B_X^{(M)} = \left| \sum_{k=1}^N \left[e_{Q_i/X_i}^{(M)} - \Psi'_X(P_i^{(LT)}, E_{0i}^{(LT)}) \right] \right| \quad (10)$$

$$R_X^{(M)} = \sqrt{\sum_{i=1}^N \left[e_{Q_i/X_i}^{(M)} - \Psi'_X(P_i^{(LT)}, E_{0,i}^{(LT)}) \right]^2} \quad (11)$$

where X is the climate variable (P or E_0), $e_{Q_i/X_i}^{(M)}$ is the corresponding empirical elasticity value computed for catchment i using sub-periods of M years, and $N = 519$ is the number of catchments.

The performance of the five alternative methods is presented in Fig. 6, which shows the absolute bias and the root mean square error on the elasticity for precipitation and potential evaporation, respectively.

The four plots in Fig. 6 clearly indicate the superiority of the two bivariate models (OLS-2 and GLS-2) over the three univariate models (NP, OLS-1 and GLS-1), with bias and RMSE on both types of elasticity that are lower by several orders of magnitude. This first result suggests that the estimation of empirical elasticity is greatly improved when conducted simultaneously on rainfall and potential evaporation.

Figure 6 also shows that the duration of the sub-periods can slightly affect the performance of the regression model. The largest impact can be seen in the bias on the elasticity to potential evaporation (Fig. 6a) where the optimal duration of 20 years provides a better performance compared to the other durations. The 20 year duration seems to be the best choice for both types of elasticity, for all regression models, and both bias and RMSE. The only noticeable exception is the bias on elasticity to rainfall (Fig. 6b) for the GLS-2 model where the best elasticity values are obtained for sub-periods of 10 years. This could indicate that the optimal duration may not be identical for the estimation of elasticity to rainfall and potential evaporation.

This study based on synthetic data shows the clear superiority of the methods based on bivariate regressions (OLS2 and GLS2): the Non-Parametric method (NP) and the univariate regressions (OLS1 and GLS1) are clearly unable to compute streamflow elasticity robustly. Because the NP method is the reference method (suggested by Sankarasubramanian et al., 2001), Fig. 7a, c compares the empirical elasticity values given by the NP method and the GLS2 method: the differences are very large. On the other hand, Fig. 7b, d shows that there is little difference between the estimates given by OLS2 and GLS2. However, for statistical reasons (presented in the Appendix) we consider that the GLS solution should be preferred.

Having decided on the best method to compute empirical elasticity, we can now compare model elasticities with the GLS estimates based on measured streamflow.

HESSD

12, 3645–3679, 2015

Climate elasticity of streamflow revisited

V. Andréassian et al.

Title Page

Abstract

Introduction

Conclusions

References

Tables

Figures



Back

Close

Full Screen / Esc

Printer-friendly Version

Interactive Discussion



4.2 Coherence of data-based and model-based elasticity estimates

We now wish to compare the *empirical* elasticity computed with the GLS2 method (the recommended one) with the *theoretical* elasticity derived analytically from the Turc–Mezentsev formula (see Eq. 3). While in the previous test we used synthetic data, we now use the actual (measured) streamflow. This means that contrary to the preceding test, we do not have any “reference”: since neither the data-based nor the model-based elasticity can be considered “true,” we can only assess the coherence between the two computations.

The scatterplots illustrated in Fig. 8 compare the elasticity values obtained by the multivariate regression (GLS2) method and the model-based approach: we can see that the link between the two measurements on a catchment-by-catchment basis remains acceptable for precipitation, but very weak for potential evaporation.

The fact that empirical and theoretical elasticities differ is in itself noteworthy and would require further analysis. At this point, we cannot draw any further conclusion from this comparison: as widely used as it is, the Turc–Mezentsev relationship remains a theoretical model and cannot be considered superior to the data-based elasticity assessment.

5 Results: regional elasticity analysis over France

Henceforth, we only consider the empirical elasticity estimates given by the GLS2 method. Figure 9 illustrates the results: each of the 519 gaging stations of the data set are shown, but the points for which the elasticity coefficient is not significantly different from zero are indicated with a cross only. For the other points, the color code gives the elasticity value.

From the maps, it is difficult to identify physical reasons for the spatial variations in elasticity values. The Massif central highlands seem to show a slightly higher occurrence of high-intensity elasticities, both to P and E_0 , and the Paris Basin low-

HESSD

12, 3645–3679, 2015

Climate elasticity of streamflow revisited

V. Andréassian et al.

Title Page

Abstract

Introduction

Conclusions

References

Tables

Figures

◀

▶

◀

▶

Back

Close

Full Screen / Esc

Printer-friendly Version

Interactive Discussion



lands a slightly lower occurrence. This tendency could perhaps be related to the absence/presence of large groundwater aquifers, but more detailed comparative studies are needed to draw a firm conclusion.

A few outliers appear, which is common when using a large data set: one catchment shows a negative elasticity to precipitation and five catchments show a positive elasticity to potential evaporation. We checked each of the plots individually and verified that this was in fact due to a very limited span of streamflow anomaly ΔQ , which made the regression rather meaningless.

To conclude this countrywide analysis of elasticity, we tested a possible relation between catchment size and elasticity values. Figure 10 speaks for itself: over the range of catchment areas covered by this study, no trend could be identified with catchment area.

6 Conclusion

6.1 Synthesis

In this paper, we identified an improved method to assess the empirical elasticity of streamflow to precipitation and potential evaporation. This method (GLS2), which uses long-term hydrometeorological records, was tested on a set of 519 French catchments.

We started with a synthetic data set and compared this improved method with the reference nonparametric method and with several univariate and bivariate alternatives: we obtained results with a much lower bias and RMSE, this difference being clearly due to the fact that the improved method was able to account for the covariation of precipitation and potential evaporation anomalies.

We then compared the improved empirical elasticity estimate with the theoretical estimates derived analytically from the Turc–Mezentsev formula. Empirical and theoretical estimates weakly correlated: the link between the two measurements on a catchment-basis is weak for precipitation, and very weak for potential evaporation.

Title Page

Abstract

Introduction

Conclusions

References

Tables

Figures

◀

▶

◀

▶

Back

Close

Full Screen / Esc

Printer-friendly Version

Interactive Discussion



6.2 Limits and perspectives

As a simple method characterizing the sensitivity of streamflow to climatic changes, the identification of empirical elasticity seems promising. Indeed, the empirical elasticity assessment advocated in this paper can provide a “model-free” estimate of the impact of climate change on hydrology, looking into past observations to predict the impact of *future* changes. Another perspective can also be seen for studies involving hydrological models for climate change assessment: empirical elasticity could provide a very useful benchmark against which to test the predictions of complex hydrological models (see e.g. how the extrapolation capacity of several hydrological models was assessed in Coron et al., 2014).

Naturally, the elasticity assessment has its limits: there is no guarantee for its ability to extrapolate to the most extreme climatic changes (i.e., to changes that are far from those observed over historical records). The formula chosen to compute potential evaporation is also a concern. In this paper, we used the Penman–Monteith equation (Allen et al., 1998). We also repeated this study with the Oudin et al. (2005) formula (a formula widely used in France), which did not yield significant differences. This result was expected because the catchments considered here are energy-limited with few cases where actual evaporation reaches its potential value. However, for other climates (i.e., drier environments), additional work would be required to test the sensitivity of streamflow elasticity to the potential evaporation formula.

Appendix: Validity of statistical assumptions underlying the regression models

This section reviews the validity of the statistical assumptions underlying the OLS2 and GLS2 regression models described in Sect. 3.3.

- Figure 11a shows that the GLS2 model has the highest proportion of catchments where the normality assumption cannot be rejected based on the Shapiro–Wilks test. However, the difference with the other models remains limited, with this pro-

HESSD

12, 3645–3679, 2015

Climate elasticity of streamflow revisited

V. Andréassian et al.

Title Page

Abstract

Introduction

Conclusions

References

Tables

Figures

◀

▶

◀

▶

Back

Close

Full Screen / Esc

Printer-friendly Version

Interactive Discussion



portion varying from 50 % for OLS2 with 10 year sub-periods to 63 % for GLS2 with 20 year sub-periods. Overall, a significant proportion of catchments still fail the test, whatever regression model is considered, which suggests that additional assumptions could be tested for the distribution of the innovations.

- 5 – Figure 11b reveals that a high level of autocorrelation is present in the innovations of the OLS2 model with only 5 % (with 10 year sub-periods) and only 27 % (with 20 year sub-periods) of the catchments reaching a satisfactory Durbin–Watson statistic value. This was an expected result. Logically, this proportion is much higher for the GLS2 models, reaching 89 % for 10 year sub-periods and 84 % for 10 year sub-periods. Here also a small proportion of the catchments fail the test, even with regression models embedding an explicit autocorrelation treatment. This result suggests that the residuals may require higher-order autoregressive models.

15 Overall, the results illustrated in Fig. 11 indicate that the GLS2 model is the most satisfactory regression model from a statistical point of view. The difference introduced by the length of the averaging period (10 or 20 years) is very limited.

The Supplement related to this article is available online at doi:10.5194/hessd-12-3645-2015-supplement.

20 *Acknowledgements.* The authors would like to acknowledge Météo-France for making the SAFRAN meteorological archive available for this study, and SCHAPI-Banque Hydro for the hydrometrical series.

Climate elasticity of streamflow revisited

V. Andréassian et al.

Title Page

Abstract

Introduction

Conclusions

References

Tables

Figures

⏪

⏩

◀

▶

Back

Close

Full Screen / Esc

Printer-friendly Version

Interactive Discussion



References

- Allen, R., Pereira, L., Raes, D., and Smith, M.: Crop evapotranspiration – Guidelines for computing crop water requirements, 100 pp., FAO, Rome, 1998.
- Arora, V. K.: The use of the aridity index to assess climate change effect on annual runoff, *J. Hydrol.*, 265, 164–177, 2002.
- Chiew, F.: Estimation of rainfall elasticity of streamflow in Australia, *Hydrol. Sci. J.*, 51, 613–625, 2006.
- Chiew, F., Potter, N. J., Vaze, J., Petheram, C., Zhang, L., Teng, J., and Post, D. A.: Observed hydrologic non-stationarity in far south-eastern Australia: implications for modelling and prediction, *Stoch. Env. Res. Risk A.*, 28, 3–15, 2014.
- Coron, L., Andréassian, V., Perrin, C., Bourqui, M., and Hendrickx, F.: On the lack of robustness of hydrologic models regarding water balance simulation: a diagnostic approach applied to three models of increasing complexity on 20 mountainous catchments, *Hydrol. Earth Syst. Sci.*, 18, 727–746, doi:10.5194/hess-18-727-2014, 2014. s
- Donohue, R., Roderick, M., and McVicar, T.: Assessing the differences in sensitivities of runoff to changes in climatic conditions across a large basin, *J. Hydrol.*, 406, 234–244, 2011.
- Dooge, J.: Sensitivity of runoff to climate change: a Hortonian approach, *B. Am. Meteorol. Soc.*, 73, 2013–2024, 1992.
- Fu, G., Charles, S. P., Viney, N. R., Chen, S., and Wu, J. Q.: Impacts of climate variability on stream-flow in the Yellow River, *Hydrol. Process.*, 21, 3431–3439, 2007.
- Johnston, J.: *Econometric Methods*, McGraw-Hill, New York, 437 pp., 1972.
- Le Moine, N., Andréassian, V., Perrin, C., and Michel, C.: How can rainfall–runoff models handle intercatchment groundwater flows? Theoretical study over 1040 French catchments, *Water Resour. Res.*, 43, W06428, doi:10.1029/2006WR005608, 2007.
- Lebecherel, L., Andréassian, V., and Perrin, C.: On regionalizing the Turc–Mezentsev water balance formula, *Water Resour. Res.*, 49, 1–10, 2013.
- Mezentsev, V.: Back to the computation of total evaporation, *Meteorol. Hydrol.*, 5, 24–26, 1955.
- Nelder, J. and Mead, R.: A simplex method for function minimization, *Comput. J.*, 7, 308–313, 1965.
- Nemec, J. and Schaake, J.: Sensitivity of water resources systems to climate variation, *Hydrolog. Sci. J.*, 27, 327–343, 1982.

HESSD

12, 3645–3679, 2015

Climate elasticity of streamflow revisited

V. Andréassian et al.

Title Page

Abstract

Introduction

Conclusions

References

Tables

Figures

⏪

⏩

◀

▶

Back

Close

Full Screen / Esc

Printer-friendly Version

Interactive Discussion



Climate elasticity of streamflow revisited

V. Andréassian et al.

Title Page

Abstract

Introduction

Conclusions

References

Tables

Figures

⏪

⏩

◀

▶

Back

Close

Full Screen / Esc

Printer-friendly Version

Interactive Discussion



Niemann, J. D. and Eltahir, A. B.: Sensitivity of regional hydrology to climate changes, with application to the Illinois River basin, *Water Resour. Res.*, 41, W07014, doi:10.1029/2004WR003893, 2005.

Oudin, L., Hervieu, F., Michel, C., Perrin, C., Andréassian, V., Anctil, F., and Loumagne, C.: Which potential evapotranspiration input for a lumped rainfall–runoff model? Part 2 – Towards a simple and efficient potential evapotranspiration model for rainfall–runoff modelling, *J. Hydrol.*, 303, 290–306, 2005.

Potter, N. J. and Zhang, L.: Interannual variability of catchment water balance in Australia, *J. Hydrol.*, 369, 120–129, 2009.

Potter, N. J., Chiew, F. H. S., and Frost, A. J.: An assessment of the severity of recent reductions in rainfall and runoff in the Murray–Darling Basin, *J. Hydrol.*, 381, 52–64, 2010.

Potter, N. J., Petheram, C., and Zhang, L.: Sensitivity of streamflow to rainfall and temperature in south-east Australia during the Millenium drought, paper presented at 19th International Congress on Modelling and Simulation, 12–16 December 2011, MSSANZ, Perth, Australia, 2011.

Sankarasubramanian, A., Vogel, R. M., and Limbrunner, J. F.: Climate elasticity of streamflow in the United States, *Water Resour. Res.*, 37, 1771–1781, 2001.

Schaake, J. and Liu, C.: Development and application of simple water balance models to understand the relationship between climate and water resources, in: *New Directions for Surface Water Modeling*, IAHS, Wallingford, 343–352, 1989.

Turc, L.: Le bilan d'eau des sols: relation entre les précipitations, l'évaporation et l'écoulement, *Ann. Agron.*, A5, 491–595, 1954.

Vogel, R. M., Wilson, I., and Daly, C.: Regional regression models of annual streamflow for the United States, *J. Irrig. Drain. E.-ASCE*, 125, 148–157, 1999.

Wolock, D. M. and McCabe, G. J.: Estimates of runoff using water-balance and atmospheric general circulation models, *J. Am. Water Resour. As.*, 35, 1341–1350, 1999.

Yang, H. and Yang, D.: Derivation of climate elasticity of runoff to assess the effects of climate change on annual runoff, *Water Resour. Res.*, 47, W07526, doi:10.1029/2010WR009287, 2011.

Yang, H., Yang, D., Lei, Z., and Sun, F.: New analytical derivation of the mean annual water–energy balance equation, *Water Resour. Res.*, 44, W03410, doi:10.1029/2007WR006135, 2008.

Yang, H., Yang, D., and Hu, Q.: An error analysis of the Budyko hypothesis for assessing the contribution of climate change to runoff, *Water Resour. Res.*, 50, 9620–9629, 2014.

HESSD

12, 3645–3679, 2015

Climate elasticity of streamflow revisited

V. Andréassian et al.

Title Page

Abstract

Introduction

Conclusions

References

Tables

Figures



Back

Close

Full Screen / Esc

Printer-friendly Version

Interactive Discussion



Climate elasticity of streamflow revisited

V. Andréassian et al.

Table 1. Summary of the elasticity notations used in this paper (X being precipitation P or potential evaporation E_0).

Notation	Definition	Formula
$\varepsilon_{Q/X}$	Relative streamflow elasticity – percent change of streamflow Q by percent change of climate variable X	$\frac{\Delta Q}{Q} = \varepsilon_{Q/X} \frac{\Delta X}{X}$
$e_{Q/X}$	Absolute streamflow elasticity – mm change of streamflow Q by mm change of climate variable X	$\Delta Q = e_{Q/X} \cdot \Delta X$

[Title Page](#)
[Abstract](#)
[Introduction](#)
[Conclusions](#)
[References](#)
[Tables](#)
[Figures](#)
[I◀](#)
[▶I](#)
[◀](#)
[▶](#)
[Back](#)
[Close](#)
[Full Screen / Esc](#)
[Printer-friendly Version](#)
[Interactive Discussion](#)


Climate elasticity of streamflow revisited

V. Andréassian et al.

Title Page

Abstract

Introduction

Conclusions

References

Tables

Figures

◀

▶

◀

▶

Back

Close

Full Screen / Esc

Printer-friendly Version

Interactive Discussion



Table 2. Comparison of the theoretical and empirical elasticity assessment methods.

	Theoretical (model-based) elasticity assessment	Empirical (data-based) elasticity assessment
Co-variations of different climatic variables	The modeling approach distinguishes between the impact of different climatic variables (by keeping part of the forcing constant while modifying the other part).	Problem: the changes in observed climatic variables can be correlated (e.g., ΔP negatively correlated with ΔT when the driest years are also the warmest), which makes it more difficult to attribute streamflow changes to one or the other variable.
Data requirements	No need for long concomitant series of observed streamflow and climatic variables (only what is needed for model calibration).	Long concomitant series of observed streamflow and climatic variables are required.
Extrapolation capacity	Extrapolates to extreme climatic changes (i.e., to changes that have not been observed over historical records).	Can only deal with the changes that have been observed in the available historical record.

Climate elasticity of streamflow revisited

V. Andréassian et al.

Table 3. Regression models used to assess empirical elasticity.

Notation	Definition	Inputs	Number of parameters
NP	Nonparametric regression	$\Delta P_i^{(M)}$ or $\Delta E_{0i}^{(M)}$	0
OLS1	Ordinary least squares using a single climate input	$\Delta P_i^{(M)}$ or $\Delta E_{0i}^{(M)}$	1
OLS2	Ordinary least squares using two climate inputs	$\Delta P_i^{(M)}$ and $\Delta E_{0i}^{(M)}$	2
GLS1	Generalized least squares using a single climate input	$\Delta P_i^{(M)}$ or $\Delta E_{0i}^{(M)}$	3
GLS2	Generalized least squares using two climate inputs	$\Delta P_i^{(M)}$ and $\Delta E_{0i}^{(M)}$	4

Title Page

Abstract

Introduction

Conclusions

References

Tables

Figures

⏪

⏩

◀

▶

Back

Close

Full Screen / Esc

Printer-friendly Version

Interactive Discussion



Climate elasticity of streamflow revisited

V. Andréassian et al.

Title Page

Abstract

Introduction

Conclusions

References

Tables

Figures

I ◀

▶ I

◀

▶

Back

Close

Full Screen / Esc

Printer-friendly Version

Interactive Discussion

**Table 4.** Univariate regression models for empirical elasticity assessment.

$$\Delta Q_i^{(M)} = e_{Q/X}^{(M)} \cdot \Delta X_i^{(M)} + \omega_i \quad \text{Eq. (12)}$$

$$\begin{array}{l} \text{OLS} \quad \omega_i \sim N(0, \sigma) \\ \text{GLS} \quad \left\{ \begin{array}{l} \omega_i = \alpha \omega_{i-1} + \delta_i \\ \delta_i \sim N(0, \sigma) \\ \omega_i \sim N(0, \sigma \sqrt{1 - \alpha^2}) \end{array} \right. \end{array}$$

$\Delta Q_i^{(M)}$: streamflow anomaly over M years, considered as the explained variable

$\Delta X_i^{(M)}$: rainfall or potential evaporation anomaly for the same sub-period, considered as the explanatory variable

$e_{Q/X}^{(M)}$: streamflow elasticity (equal to the regression slope)

ω_i : regression residual

α : parameter of the first-order autoregressive process (AR1)

δ_i : innovation of the autoregressive process

σ : SD

M : number of years over which the long-term streamflow, precipitation and evaporation average is computed



Figure 1. Location of the 519 French catchments analyzed in this study.

HESD

12, 3645–3679, 2015

Climate elasticity of streamflow revisited

V. Andréassian et al.

Title Page

Abstract

Introduction

Conclusions

References

Tables

Figures



Back

Close

Full Screen / Esc

Printer-friendly Version

Interactive Discussion



Climate elasticity of streamflow revisited

V. Andréassian et al.

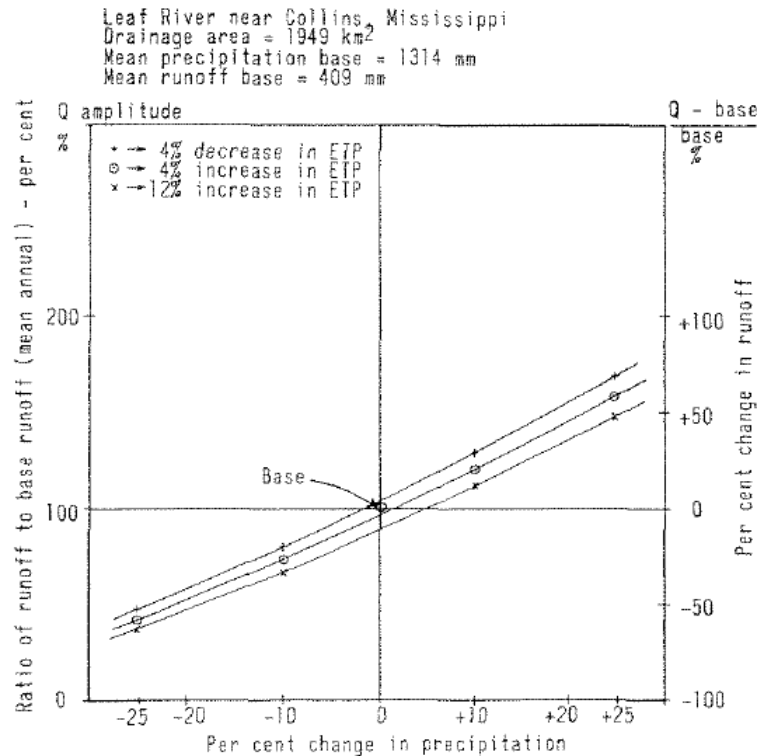


Figure 2. Yield change graph proposed by Nemeč and Schaake (1982) to illustrate the hydrological elasticity analysis.

[Title Page](#)

[Abstract](#) | [Introduction](#)

[Conclusions](#) | [References](#)

[Tables](#) | [Figures](#)

[I ◀](#) | [▶ I](#)

[◀](#) | [▶](#)

[Back](#) | [Close](#)

[Full Screen / Esc](#)

[Printer-friendly Version](#)

[Interactive Discussion](#)



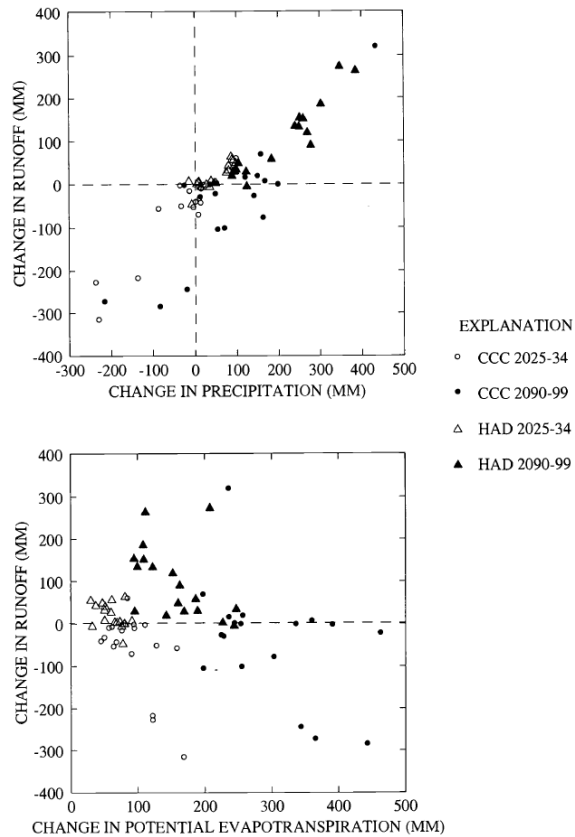


Figure 3. Elasticity graphs proposed by Wolock and McCabe (1999).

[Title Page](#)

Abstract	Introduction
Conclusions	References
Tables	Figures

[◀](#)
[▶](#)

[◀](#)
[▶](#)

[Back](#)
[Close](#)

[Full Screen / Esc](#)

[Printer-friendly Version](#)

[Interactive Discussion](#)



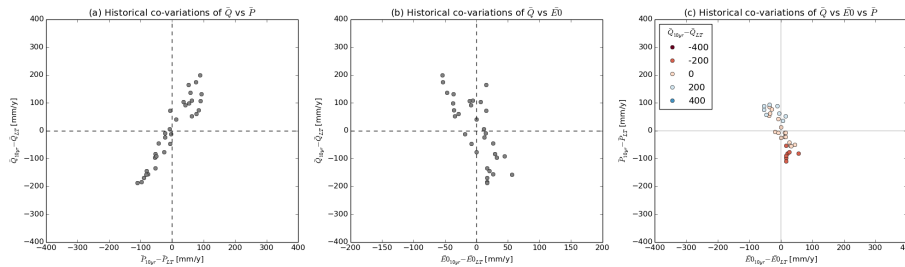


Figure 4. Streamflow elasticity graphs for an empirical (data-based) assessment for the Brèze catchment at Meyrueis (code: O3165010): **(a)** ΔQ vs. ΔP , **(b)** ΔQ vs. ΔE_0 , **(c)** ΔQ (color-coded) vs. ΔP and ΔE_0 .

Title Page

Abstract

Introduction

Conclusions

References

Tables

Figures

◀

▶

◀

▶

Back

Close

Full Screen / Esc

Printer-friendly Version

Interactive Discussion



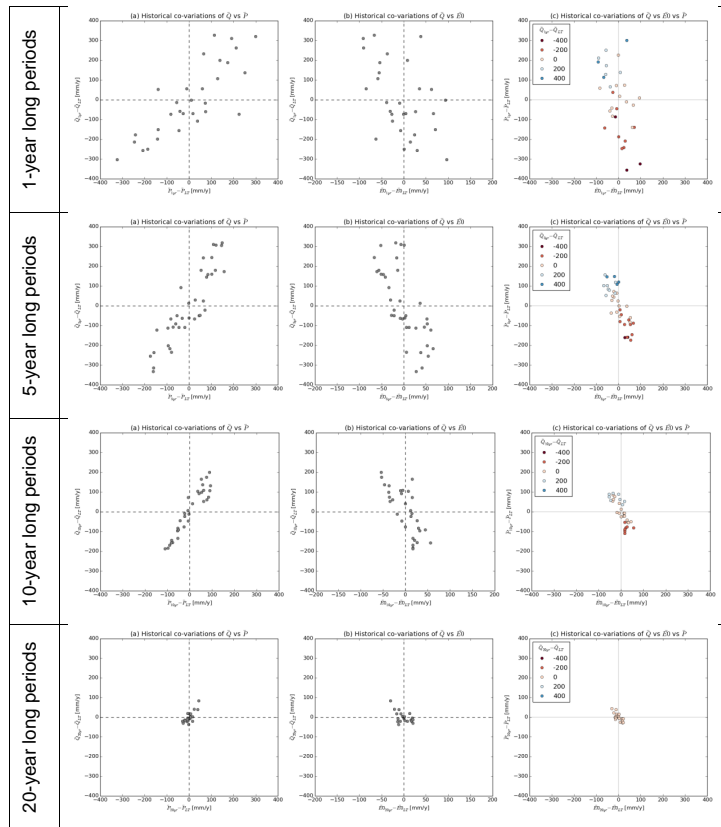


Figure 5. Impact of period length on the streamflow elasticity graphs for an empirical (data-based) assessment. The graphs present from left to right ΔQ vs. ΔP , ΔQ vs. ΔE_0 , ΔQ (in colors) vs. ΔP and ΔE_0 . LT stands for long term (entire period).

Title Page

Abstract

Introduction

Conclusions

References

Tables

Figures



Back

Close

Full Screen / Esc

Printer-friendly Version

Interactive Discussion



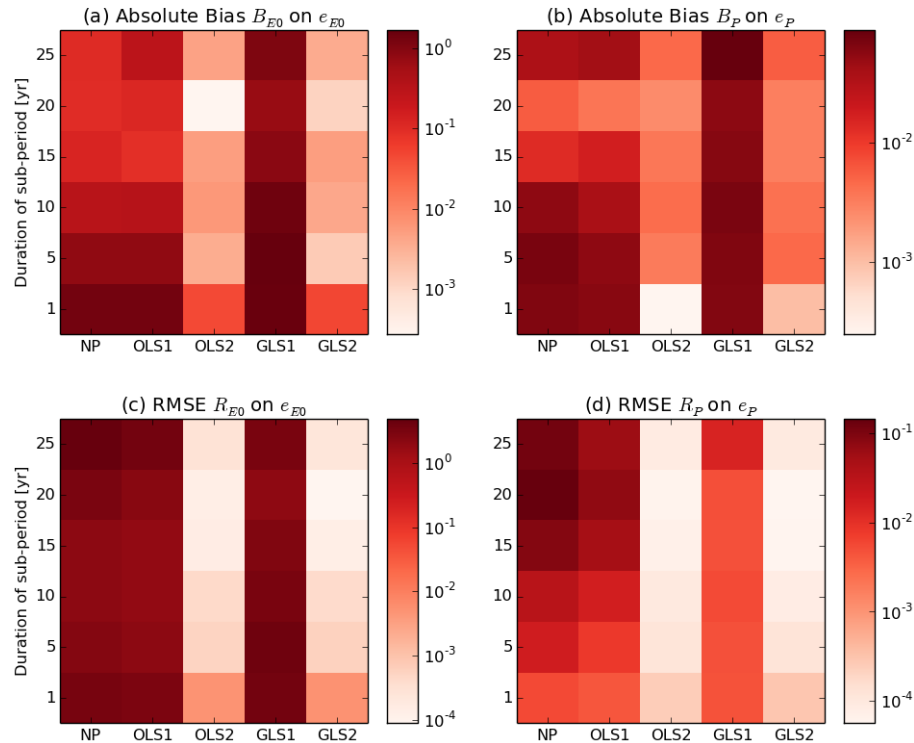


Figure 6. Performance of the five models proposed to compute empirical elasticity, tested on synthetic data generated with the Turc–Mezentsev model.

[Title Page](#)
[Abstract](#)
[Introduction](#)
[Conclusions](#)
[References](#)
[Tables](#)
[Figures](#)
[⏪](#)
[⏩](#)
[◀](#)
[▶](#)
[Back](#)
[Close](#)
[Full Screen / Esc](#)
[Printer-friendly Version](#)
[Interactive Discussion](#)

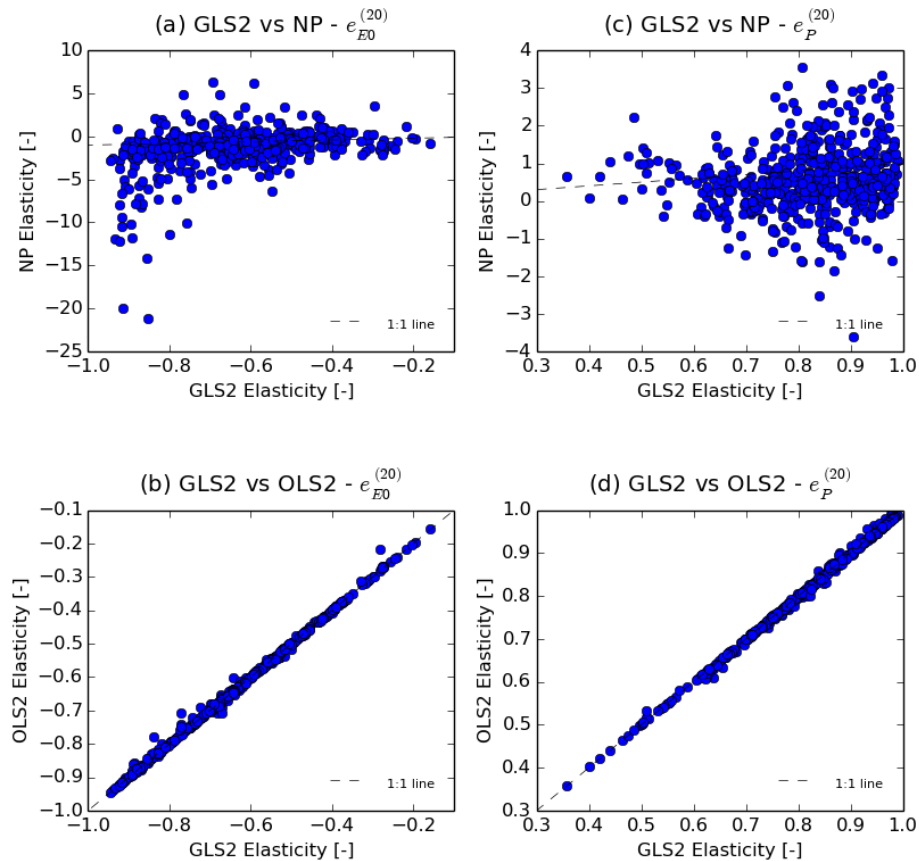



Figure 7. Comparison of elasticity estimates obtained with the GLS2, OLS2 and NP methods using synthetic flow data and 20 year sub-periods.

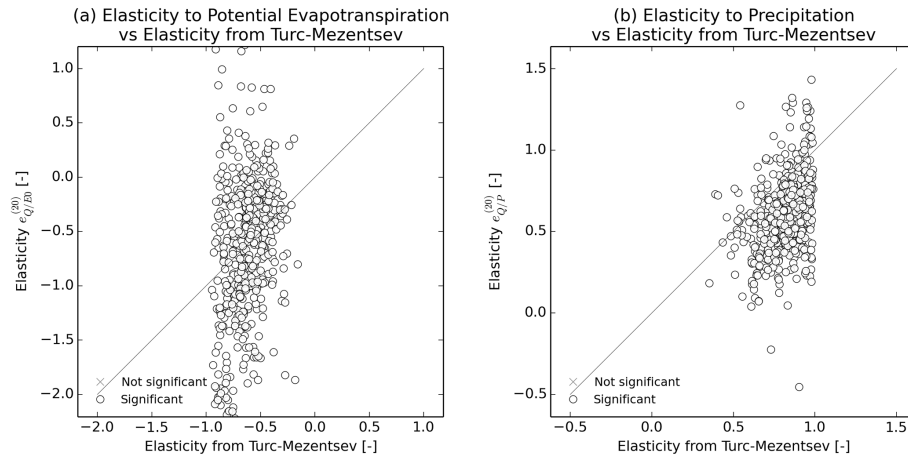


Figure 8. Comparison of the data-based and model-based elasticities; streamflow elasticity to potential evaporation **(a)** and precipitation **(b)**.

[Title Page](#)[Abstract](#)[Introduction](#)[Conclusions](#)[References](#)[Tables](#)[Figures](#)[◀](#)[▶](#)[◀](#)[▶](#)[Back](#)[Close](#)[Full Screen / Esc](#)[Printer-friendly Version](#)[Interactive Discussion](#)

Climate elasticity of streamflow revisited

V. Andréassian et al.

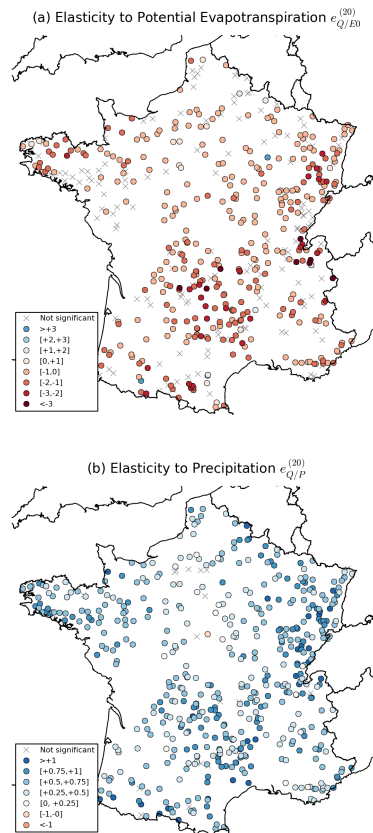


Figure 9. Regional analysis of (a) streamflow elasticity to precipitation and (b) streamflow elasticity to potential evaporation. Elasticity values were obtained by the GLS2 regression method using 20 year sub-periods. Each dot represents a catchment outlet, the color represents the elasticity value. Those catchments where the linear correlation was found to be nonsignificant are indicated with a cross.

Climate elasticity of streamflow revisited

V. Andréassian et al.

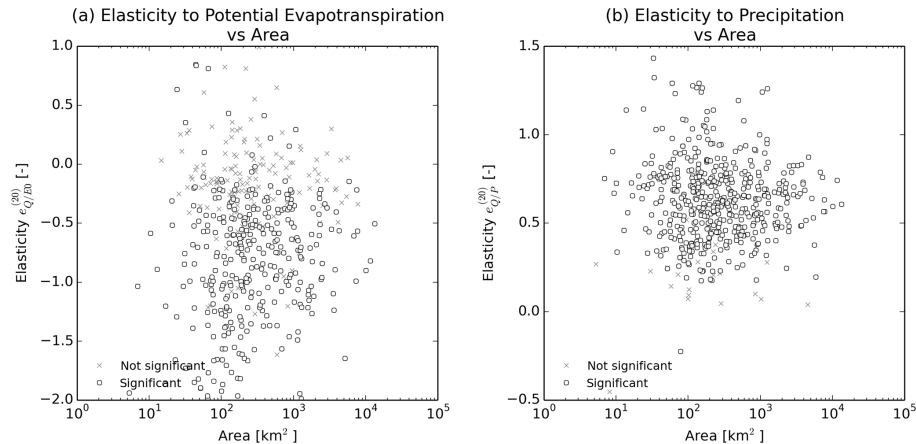


Figure 10. Elasticity values vs. catchment area: **(a)** streamflow elasticity to potential evaporation and **(b)** streamflow elasticity to precipitation. Elasticity values were obtained by the GLS2 regression method with 20 year sub-periods.

Title Page

Abstract

Introduction

Conclusions

References

Tables

Figures

◀

▶

◀

▶

Back

Close

Full Screen / Esc

Printer-friendly Version

Interactive Discussion



